



Published in final edited form as:

*Exp Neurol.* 2009 January ; 215(1): 119–127. doi:10.1016/j.expneurol.2008.09.024.

## Immediate Short-Duration Hypothermia Provides Long-Term Protection in an in Vivo Model of Traumatic Axonal Injury

Marek Ma, MD<sup>1,3</sup>, Brian T. Matthews, BA<sup>1,3</sup>, Joshua W. Lampe, PhD<sup>1,3</sup>, David F. Meaney, PhD<sup>2</sup>, Frances S. Shofer, PhD<sup>1,4</sup>, and Robert W. Neumar, MD, PhD<sup>1,3</sup>

<sup>1</sup>Department of Emergency Medicine, University of Pennsylvania, Philadelphia, PA

<sup>2</sup>Department of Bioengineering, University of Pennsylvania, Philadelphia, PA

<sup>3</sup>Center for Resuscitation Science, University of Pennsylvania, Philadelphia, PA

<sup>4</sup>Department of Clinical Studies, School of Veterinary Medicine, University of Pennsylvania, Philadelphia, PA

### Abstract

A prospective, multicenter, randomized trial did not demonstrate improved outcomes in severe traumatic brain injured patients treated with mild hypothermia (Clifton, et al., 2001). However, the mean time to target temperature was over 8 hours and patient inclusion was based on Glasgow Coma Scale score so brain pathology was likely diverse. There remains significant interest in the benefits of hypothermia after traumatic brain injury (TBI) and, in particular, traumatic axonal injury (TAI), which is believed to significantly contribute to morbidity and mortality of TBI patients. The long-term beneficial effect of mild hypothermia on TAI has not been established. To address this issue, we developed an in vivo rat optic nerve stretch model of TAI. Adult male Sprague-Dawley rats underwent unilateral optic nerve stretch at 6, 7 or 8 mm piston displacement. The increased number of axonal swellings and bulbs immunopositive for non-phosphorylated neurofilament (SMI-32) seen four days after injury was statistically significant after 8 mm displacement. Ultrastructural analysis 2 weeks after 8 mm displacement revealed a 45.0% decrease ( $p < 0.0001$ ) in myelinated axonal density in the optic nerve core. There was loss of axons regardless of axon size. Immediate post-injury hypothermia (32°C) for 3 hours reduced axonal degeneration in the core ( $p = 0.027$ ). There was no differential protection based on axon size. These results support further clinical investigation of temporally optimized therapeutic hypothermia after traumatic brain injury.

### Keywords

diffuse axonal injury; trauma; optic nerve; brain injury; hypothermia

### Introduction

Currently, there are up to 6.5 million people in the United States living with the devastating physical, cognitive, and economic costs of traumatic brain injury (TBI) (NIH Consensus

---

Address for correspondence: Marek Ma, MD, Department of Emergency Medicine, University of Pennsylvania, 3400 Spruce Street, Ground Ravdin, Philadelphia, PA 19104, Tel (215) 662-4025, Fax (215) 662-3953, mamarek@uphs.upenn.edu.

**Publisher's Disclaimer:** This is a PDF file of an unedited manuscript that has been accepted for publication. As a service to our customers we are providing this early version of the manuscript. The manuscript will undergo copyediting, typesetting, and review of the resulting proof before it is published in its final citable form. Please note that during the production process errors may be discovered which could affect the content, and all legal disclaimers that apply to the journal pertain.

Development Panel on Rehabilitation of Persons with Traumatic Brain injury, 1999). An estimated 1.5 to 2 million cases of TBI occur each year in the US. It is predicted by the year 2020, TBI will be the third leading cause of death and disability each year in the world (Murray and Lopez, 1997). Traumatic axonal injury (TAI) contributes to the high rate of morbidity and mortality seen in severe TBI patients without space occupying lesions (Gennarelli, et al., 1982; Büki, et al., 2000). TAI is also believed to contribute to neurologic dysfunction after mild TBI.

Studying TAI in the brain in vivo is complex as the traumatic event may proximately damage nuclei, dendritic fields, nerve tracts, and vasculature. The interplay between the various brain structures does not allow the investigator to isolate the specific mechanism and consequences of TAI. Direct injury to neuronal cell bodies and their dendritic fields, or glial cells and vasculature could have secondary effects on axons. Hemorrhage, elevated intracranial pressure and secondary ischemia are common after severe TBI, and are associated with poorer outcome. The difficulty in identifying specific neuronal cell bodies, which give rise to the axons of interest, limits experimental manipulation and interpretation. These limitations can be overcome in the optic nerve stretch model. The optic nerve shares similar properties with white matter tracts within the brain, including poor regenerative capacity, myelin sheath structure, and the presence of oligodendrocytes (Hirano and Lena, 1995; Cho, et al., 2005).

In both humans and animals, trauma produces a rapid elongation of axons that generally does not cause primary axotomy (immediate tearing of the axon) but leads to progressive structural damage culminating in secondary axotomy (Jafari, et al., 1997; Maxwell and Graham, 1997; Povlishock, et al., 1997; Saatman, et al., 2003; Povlishock and Katz, 2005). The distinction between primary and secondary axotomy is critical as primary axotomy in the CNS is considered irreversible. Impairment of axonal transport with subsequent accumulation of transported proteins and organelles, visualized using antibodies targeting amyloid precursor protein (APP) or neurofilament, are hallmarks of TAI. These sites of accumulated transported materials are known as axonal swellings. Eventually, a constriction may form near the swelling that progresses to axonal disconnection. This terminal increase in axonal diameter found after axonal disconnection is termed axonal bulb.

Posttraumatic hypothermia has previously been shown to afford short-term axonal protection in models of TAI. Hypothermia (32.0-32.5°C) induced immediately and maintained for 4 hours after guinea pig optic nerve stretch reduced the number of  $\beta$ -APP labeled axons in animals sacrificed 4 and 8 hours after injury (Maxwell, et al., 1999; Maxwell, et al., 2005). Both studies also demonstrated preservation of cytoskeletal ultrastructure with hypothermia. Twenty-four hours after impact acceleration head injury in rats, there was a reduction in the number of APP-labeled axons with 1 hour of hypothermia (32°C) induced immediately after injury (Koizumi and Povlishock, 1998). Collectively, these past studies demonstrate the promise of using immediate mild hypothermia in mitigating TAI. However, the long-term benefits of hypothermia remain relatively unexplored. The previous studies counted APP-labeled axons, but this may significantly underestimate the overall magnitude of the axonal damage caused by trauma (Povlishock and Katz, 2005). It is not known whether all APP-labeled axons ultimately degenerate.

To address this issue, we developed a rat model of in vivo optic nerve stretch and demonstrated pathology similar to that observed in human TBI. Furthermore, we report for the first time sustained axonal preservation with immediate short-duration hypothermia after isolated axonal stretch injury in vivo.

## Materials and Methods

All animal procedures were performed in accordance with NIH guidelines for the care and use of laboratory animals and were approved by our Institutional Animal Care and Use Committee.

### Surgical Preparation for Optic Nerve Stretch

Adult male Sprague-Dawley rats (weight 300-400 grams) underwent general anesthesia with 2.5% isoflurane and were placed on a heating pad for surgery. Anesthesia was maintained via a nose cone. The cornea was anesthetized with 0.5% proparacaine, and the eye was kept moist at all times using sterile saline. The conjunctiva was separated from the sclera using an incision extending around the entire circumference of the eye except for the medial aspect (to minimize bleeding). A flexible thin ring-shaped plastic sling, which had a continuous loop of 4-0 monofilament nylon suture secured to it at two places 180° apart, was placed behind the eye. The sling had a break in its ring so the ends could be spread apart to allow placement behind the eye, and, after placement, the two ends of the ring were sutured together. The monofilament nylon loop was then attached to the optic nerve stretch device.

### Rat Optic Nerve Stretch

To receive optic nerve injury, rats were placed in a stereotactic head holder that was positioned on the injury device (modified from Gennarelli, et al., 1989). We used rats, rather than mice, for these experiments because of the larger anatomic dimensions of the optic nerve, which allows for more precise control of the biomechanics of injury. For experiments characterizing SMI-32 immunohistochemistry, rectal temperature was used. For all other experiments, a probe placed in the temporalis muscle was used as a surrogate for brain temperature and was maintained at 37.0–37.5°C at the time of injury. The head was positioned on the injury device such that the trajectory of the retro-orbital portion of the optic nerve was aligned with the stroke of the solenoid. The sling was connected to a force transducer (ELF T5000-a; Entran, Fairfield, NJ) mounted in series with a solenoid (Lucas-Ledex, Vandalia, OH) and in parallel with a displacement transducer (Trans-Tek Inc., Ellington, CT). To ensure consistent loading, a 30 g preload, measured by the force transducer, was placed on the nerve. The magnitude of the displacement was controlled by a micromanipulator that adjusts the distance traveled by the solenoid piston. Preliminary experiments in freshly sacrificed animals (part of the forebrain was removed so that the optic nerve was visualized during stretch) suggested that the distance the piston traveled was significantly more than the actual stretch of the optic nerve, consistent with past experiments in the guinea pig (Bain and Meaney, 2000). The magnitude of optic nerve stretch reported here refers to piston displacement. Immediately after obtaining the preload, the solenoid was triggered to produce a rapid elongation of the nerve. For 8 mm piston displacement, the nerve was extended to the maximum displacement, held briefly, and then returned to its original pre-injury position within 75 milliseconds of initially activating the solenoid. For the experiments in this report, the peak displacement occurred 25 milliseconds after triggering the solenoid, which is consistent with the timing of peak deformation that occurs within the brain during conditions that cause diffuse axonal injury (Meaney, et al., 1995). The plateau force, which was measured when the optic nerve was elongated to its maximum length, ranged from approximately 220 to 360 grams after accounting for the initial preload.

Animals were excluded if injury to the globe or tearing of the optic nerve was apparent by visual inspection. In a subset of animals without obvious injury to the globe or optic nerve, pupils were dilated with 1% tropicamide for indirect fundoscopic evaluation, which revealed normal retinal vessels without retinal hemorrhage, and rarely minimal intravitreal bleeding.

The contralateral uninjured eye was used as a control. Sham surgery was performed on both optic nerves of two animals exactly as described except the solenoid was not triggered. All

animals were recovered on a heating pad until the animal awakened from anesthesia, which usually took less than 5 minutes.

## Hypothermia

All animals were subjected to unilateral 8 mm optic nerve stretch at normothermia (temporalis temperature between 37.0 and 37.5°C). The contralateral optic nerves in each animal served as controls. In the experimental group, hypothermia was induced immediately after stretch by fan, cold water spray and ice packs, and the animal was maintained at 32°C for 3 hours. Animals were then slowly rewarmed 1°C every 40 minutes to a temperature of 37°C before ending general anesthesia. The rewarming rate was selected based on a study by Maxwell, et al. (2005). Control animals were maintained at 37.5°C and kept anesthetized (1-1.5% isoflurane by a nose cone) for the same duration as the hypothermic animals.

## Bright Field Microscopy

**Tissue processing**—Four days after optic nerve stretch, rats, under deep isoflurane anesthesia, were perfused transcardially with cold 1× PBS followed by cold 4% paraformaldehyde in 0.1 M phosphate buffer. The optic nerves and eyes were exposed by dissection and separately removed from the head. Nerves were postfixed overnight before cryoprotection in 30% sucrose.

### Immunohistochemistry of optic nerves for conventional bright field microscopy

—Optic nerves were cut longitudinally into 10 µm thick sections on a freezing sliding microtome. Nerve sections were mounted on microscope slides and allowed to dry over several days. Slides were rinsed in an ethanol series, pretreated in 5% H<sub>2</sub>O<sub>2</sub> and 83% methanol for 30 minutes at room temperature, and rinsed in 1× PBS. Sections were blocked in 3% goat serum and 0.1% triton x-100. The tissue sections were incubated overnight at 4°C with SMI-32 (1:2000; Sternberger Monoclonals Inc., Lutherville, MD, USA), which reacts with a non-phosphorylated epitope in neurofilament H. Accumulation of neurofilament highlights axonal swellings and bulbs. Mounted sections were then incubated with biotinylated goat anti-mouse secondary antibody (1:600) for 1 hour at room temperature. The enzymatic reaction was visualized using 3, 3' diaminobenzidine tetrahydrochloride. Slides were rinsed in xylene and coverslipped with DPX.

## Electron Microscopy

**Tissue processing**—Fourteen days after optic nerve stretch, rats, under deep isoflurane anesthesia, were perfused transcardially with 1× PBS followed by 2% paraformaldehyde and 2% glutaraldehyde in 0.1 M sodium cacodylate. Solutions were at room temperature. The brain was removed and the optic nerves were left in situ and postfixed overnight at 4°C. The optic nerves were then dissected from the skull, and allowed to remain in postfix until ready for processing. Nerves were ossicated, dehydrated in ethanol and propylene oxide. The prechiasmatic region of the optic nerve was embedded in epoxy resin and oriented specifically for cross-sections of the axons. Eighty nm thick sections were stained with uranyl acetate and bismuth subnitrite for ultrastructural analysis. One section from each nerve was analyzed for quantification of myelinated axons.

## Assessment of Histological Outcomes

**A. Axonal accumulation of non-phosphorylated neurofilament (SMI-32)**—Every eighth longitudinal section of the optic nerve (10 µm thick) was mounted on slides and dried for several days. The sections were labeled for SMI-32 as described above. Using a Leica DM4500B, 100× images of each section was captured by CCD camera. The number of discrete swellings and bulbs (diameter larger than 2.5 microns) in each mounted longitudinal section

(starting from behind the eye to the optic chiasm) at a final magnification of 200× was counted by two independent blinded observers (except for sham injured nerves which were scored by one observer) (Figure 1). The total number of swellings and bulbs per each optic nerve was determined by each observer. The area of each mounted longitudinal section was calculated using NIH ImageJ and summed to get the total area scored. The number of swellings and bulbs per square mm was calculated for each optic nerve. Reported values for each nerve are the mean of two observers.

**B. Quantification of Myelinated Axons**—Optic nerve sections prepared for transmission electron microscopy were imaged using a JEOL JEM 1010 electron microscope aided by AMT HR-12 software and Hamamatsu CCD camera. An outline of the optic nerve cross-section was made and the x,y coordinates for the most superior and leftward points of the nerve border was recorded. The starting point for image capture was determined using the x from the most leftward coordinate and y from the most superior coordinate (Figure 2). Images were taken every 70 microns across until the rightward edge of the optic nerve was reached. The camera was then moved 70 microns down, and images every 70 microns across the optic nerve were taken. This process was repeated until the entire optic nerve was systematically sampled (about 2% of the total area).

A counting frame was then overlay on each image (final magnification of 13,900×), and a blinded observer counted the number of myelinated axons that had some preservation of ultrastructure. We did not count unmyelinated axons as they comprise less than 1% of total axons in the rat optic nerve (Sugimoto et al., 1984). The area of the optic nerve was calculated using NIH imageJ, and axon counts were extrapolated so that total axons per optic nerve are reported.

Each image had known x, y coordinates. The coordinates of all images from each optic nerve were plotted, and an ellipse was statistically fitted to the plot of the image coordinates. An ellipse can be described by the length of its major and minor axes. The length of the axes of the ellipse that result from the fit to the coordinate data represents the standard deviation of the data in the coordinate plane where the origin of the plane and the geometric center of the ellipse are coincident, and the major and minor axes are colinear with the axes of the coordinate system. To determine the scaled distance (i.e. percent) from the geometric center, an affine transform was performed and the coordinate system was scaled so that the ellipse becomes a circle (Figure 3). An affine transformation was performed in order to compensate for the varying aspect ratios (length of minor axis:length of major axis) of optic nerve cross-sections. In addition, it compensated for the different spatial orientation (location of centroid and rotation) of nerve cross-sections by statistically fitting the ellipse. The distance from the geometric center in the scaled coordinate system was used to rank the images. Images nearest to the center were considered be taken from the nerve center, while the rest of images were considered to be taken from the nerve periphery. Images were evenly divided between center and periphery. When there were an odd number of images for a nerve, the additional image was classified as central. Axon densities are reported.

**C. Axon cross-sectional area**—A counting frame was overlay on each image taken from the central region of each optic nerve (final magnification of 13,900×). Using Adobe Photoshop® CS3 Extended (v 10.0.1), a blinded observer used the quick selection tool to outline the axoplasmic area of each myelinated axon. The cross-sectional areas of approximately 220-300 axons in the uninjured nerves and 40-280 in injured nerves were calculated. The axons in each uninjured normothermic optic nerve were divided into quartiles based on cross-sectional area. Using only the normothermic uninjured nerves, the mean 25<sup>th</sup>, 50<sup>th</sup>, and 75<sup>th</sup> percentiles were established, and these values were subsequently used to separate the axons from the 24 optic nerves into four quartiles. The mean density of axons (6 optic

nerves in each group) in each quartile is reported. The first quartile represent the smallest axons, while the fourth quartile represent the largest axons.

### Statistical Analysis

The percentage axonal loss (the percent difference in axon number between the injured and its contralateral control optic nerve) between the normothermic and hypothermic groups was compared using a Student's t-test. All other analyses were performed using analysis of variance (ANOVA) in repeated measures. A p-value <0.05 for main effects and <0.2 for the interaction term was considered statistically significant. Post-hoc pairwise comparisons were accomplished using the t-test with pooling of the variance. Significance levels for post-hoc comparisons were adjusted for by using the Bonferroni correction. These levels varied depending on the number of preplanned pairwise comparisons made. Data are presented as means and standard deviation. All analyses were performed using SAS statistical software (Version 9.1, SAS Institute, Cary NC).

## Results

### Immunohistochemical analysis of axonal injury

In our preliminary experiments, 10 mm of stretch consistently tore the optic nerve. We therefore decided to compare number of axonal swellings and bulbs four days after 6, 7 and 8 mm of stretch (SEVERITY, n=3 animals per group). Overall, there was a significant INJURY effect ( $F=21.8$ ,  $p=0.003$ ) as well as an interaction (INJURY\*SEVERITY,  $F=2.3$ ,  $p=0.186$ ). Because we wanted to determine a level of stretch severity that produced axonal injury, there were three pre-planned comparisons: each injury severity with their respective contralateral control nerves. A  $p<0.016$  was considered significant. Axonal swellings and bulbs highlighted by SMI-32 labeling were detected after all three injury severities with 8 mm stretch reaching statistical significance relative to contralateral control nerves ( $p=0.009$ ) (Figures 4 and 5). Injury was detected throughout the nerve, but was mainly concentrated at the prechiasmatic segment. In a separate experiment, the mean number ( $\pm$ SD).of swellings and bulbs per square mm 4 days after sham surgery were  $1.04\pm 1.07$ .

### Hypothermia as a strategy for axonal protection after trauma

**Overall axonal loss**—Twelve rats (n=6 in both normothermia and hypothermic groups) were subjected to unilateral 8 mm optic nerve stretch at normothermia. Right optic nerves served as uninjured controls. In the TREATMENT group, hypothermia was immediately induced after stretch. Target temperature of 32°C was reached at a mean ( $\pm$ SD) time of 16.4  $\pm$ 1.8 minutes. An interim target of 34°C was reached at 10.8 $\pm$ 2.0 minutes.

Fourteen days after injury, rats were euthanized by perfusion fixation and optic nerve cross sections were prepared for transmission electron microscopy. There was a significant INJURY effect ( $F=20.4$ ,  $p=0.001$ ) and an interaction (INJURY\*TREATMENT,  $F=1.90$ ,  $p=0.198$ ). There were three pre-planned comparisons: injured versus control nerves in normothermic animals, injured versus control nerves in hypothermic animals, and normothermic injured versus hypothermic injured nerves. A  $p<0.016$  was considered significant. The number of myelinated axons was  $89214\pm 3348$  and  $86485\pm 4286$  in normothermic and hypothermic control nerves, respectively. In injured optic nerves, the number of myelinated axons was  $56220\pm 19090$  (37.1% decrease,  $p=0.002$ ) in the normothermic group and  $68922\pm 20879$  (20.4% decrease,  $p=0.051$ ) in the hypothermic group (Figures 6 and 7A). The mean number of axons in hypothermic and normothermic injured nerves was not statistically different ( $p=0.14$ ). Likewise, the overall percentage axonal loss after injury (pairing each injured optic nerve to its contralateral uninjured optic nerve) between the normothermic and hypothermic groups was not statistically different ( $p=0.14$ ) (Figure 7B).

**Regionalization of stretch injury**—Based on our histologic observations, stretch injury appeared to cause axonal degeneration disproportionately in the central region of the nerve, leaving the periphery relatively preserved. Among normothermic animals, there was an INJURY effect ( $F=10.8$ ,  $p=0.008$ ) and an interaction (INJURY\*REGION,  $F=10.5$ ,  $p=0.01$ ). There were two pre-planned comparisons, and  $p<0.025$  was considered significant. We found, in normothermic animals, a statistically significant decrease in axonal density in the central region (45.0%,  $p<0.0001$ ), but not periphery (16.6%,  $p=0.049$ ) after 8 mm optic nerve stretch (Figure 8). We therefore decided to determine if immediate short-duration hypothermia was axonal protective in the optic nerve core after stretch. Comparing core axonal density between the normothermic and hypothermic injured nerves, only an interaction effect was noted (TREATMENT\*REGION,  $F=3.64$ ,  $p=0.086$ ). There was one pre-planned comparison, and  $p<0.05$  was considered significant. Hypothermia protected against axonal loss in the optic nerve core 2 weeks after optic nerve stretch ( $p=0.027$ ).

**Injury and hypothermic protection based on axon size**—In normothermic rats, the mean percent decrease in axon density after optic nerve stretch was 38.5%, 37.2%, 37.7%, and 63.2% in the first, second, third and fourth quartiles, respectively (Figure 9). There was an INJURY effect ( $F=10.20$ ,  $p=0.024$ ) but not a QUARTILE effect ( $F=1.80$ ,  $p=0.190$ ) or an interaction (INJURY\*QUARTILE,  $F=1.04$ ,  $p=0.401$ ). Stretch injury resulted in loss of axons regardless of axon size. Comparing hypothermic to normothermic animals, there was an interaction (INJURY\*TREATMENT) effect for quartiles 2 ( $F=2.85$ ,  $p=0.122$ ) and 4 ( $F=3.40$ ,  $p=0.095$ ) but not for quartiles 1 ( $F=1.68$ ,  $p=0.212$ ) or 3 ( $F=0.00$ ,  $p=0.991$ ). However, post-hoc comparisons did not reveal any statistically significant difference between normothermic versus hypothermic injured nerves. Despite an overall treatment effect in the optic nerve core with hypothermia, there was no statistical difference between normothermic versus hypothermic injured nerves in any of the four quartiles.

## Discussion

Rat optic nerve stretch is a potentially powerful model to study the mechanism of TAI that occurs in human TBI. Our model replicates histopathologic outcomes, including SMI-32-labeled swellings and bulbs and axonal loss, seen in human TBI, and may possibly be used to study mild and severe TAI. Using this model, we were able to demonstrate robust regional long-term axonal protection with short-duration hypothermia initiated immediately after injury. The purpose of this investigation was primarily mechanistic. Our goals were to demonstrate that an intervention performed after trauma can provide long-term axonal protection, and that secondary axotomy is preventable. Defining the therapeutic window for post-injury hypothermia is a goal for future investigations.

### Our model replicates human pathology seen after TBI

The characteristics of axonal injury and degeneration seen after optic nerve stretch mimic those found in established whole brain models of axonal injury, as well as in human brain after TBI. Axonal swellings and bulbs are hallmarks of TAI. In the rodent impact acceleration head injury model, APP, which undergoes anterograde transport like neurofilament, immunoreactivity was seen in the corticospinal tract and medial longitudinal fasciculus in injured rats (Büki, et al., 2003). Nonimpact rotational acceleration in primates and pigs resulted in axonal swellings and bulbs diffusely in white matter (Gennarelli, et al., 1982; Chen, et al., 1999).

The pathology seen in the optic nerve stretch model also recapitulates what is seen in mild and severe TBI in humans. Using antibodies targeting neurofilament (including SMI-32), Grady, et al. (1993) demonstrated the progression from axonal swellings to bulbs in white matter in TBI patients. APP accumulations had been demonstrated within axons of the corpus callosum

after severe TBI (McCracken, et al., 1999). In addition, APP immunoreactive axonal swellings were described in the corpus callosum, fornices, brainstem, and subcortical white matter in mild TBI patients who died of other causes (Blumbergs, et al., 1994). Degeneration and atrophy of the fornices and corpus callosum as measured using magnetic resonance imaging have also been described (Levin, et al., 1990; Gale, et al., 1993).

There may be an injury dose response in our model. There was a mean of 82.6 swellings and bulbs per square mm after 8 mm optic nerve stretch, but only 22.0 after 6 mm stretch and 1.2 in control nerves. With 3 animals in each group, several of the post-hoc comparisons were not statistically different. Increasing our sample size may allow us to demonstrate statistically different injury dose responses. This may allow for the study of therapeutic intervention after mild and severe TAI with our model.

### **Post-injury hypothermia provides long-term protection after TAI**

Posttraumatic hypothermia had previously been shown to afford short-term axonal protection in models of TAI (Koizumi and Povlishock, 1998; Maxwell, et al., 1999; Maxwell, et al., 2005). The therapeutic benefit of hypothermia was demonstrated as late as 8 hours after guinea pig optic nerve stretch (Maxwell, et al., 2005) and as late as 24 hours after rat impact head acceleration injury (Koizumi and Povlishock, 1998). Both studies quantified APP-labeled axons but it is not known whether anterograde transport disruption is reversible or whether all APP-labeled axons must degenerate. In one study, Brodhun, et al. reported that early posttraumatic hypothermia was not axonal protective in juvenile pigs subjected to fluid percussion injury and hypovolemic hypotension. However, based on the graphical presentation of their data, the mean number of APP-labeled axons in the normothermic injured animals without elevated intracranial pressure (ICP) was more than double that of hypothermic animals (none experienced elevated ICP). Therefore, this study may have lacked adequate power to detect a treatment effect.

We are the first to determine that axonal protection seen with short-term hypothermia is preserved long-term after accounting for the regionalization of injury after optic nerve stretch. We were unable to detect a statistically significant difference in total axonal counts 2 weeks post-stretch between normothermic animals and those treated with short-duration hypothermia in spite of a mean 17% absolute reduction in axon loss with hypothermia. We believe our inability to detect a statistical difference was due to the large intra-group variability in total axonal counts and the relative concentration of injury in the optic nerve core. When regional density of myelinated axons was compared, post-injury hypothermia reduced axonal loss in the nerve core.

It is unclear why the central region of the optic nerve is preferentially injured. Maxwell, et al. (1999) had earlier reported that  $\beta$ -APP immunolabeling occurred exclusively in the central 30% of the guinea pig optic nerve after stretch. Solid mechanics dictates that homogenous, isotropic materials have a uniform stress distribution under axial loading. However, the optic nerve is neither isotropic nor homogenous. Past work showed that the microstructure of the optic nerve leads to nonlinear behavior of the structure as it is gradually elongated (Bain, et al., 2003; Meaney, 2003). One key parameter in this nonlinear behavior is the gradual straightening of the axons during slow extension, which leads to an increase in the fraction of axons bearing mechanical load at higher elongations. One possible mechanical reason for the differential injury pattern in our study is the change in axonal microstructure between the periphery and the core. Future data on the regional changes in the microstructure within the rat optic nerve would clarify if this were a contributing factor for this observation.

It is not clear if TBI preferentially injures larger caliber axons as more recent studies have suggested otherwise (Povlishock, 1992). However, different size axons appear to respond

differently to injury. In the guinea pig optic nerve stretch model, small and large axons have different responses 4 hours after injury (Jafari, et al., 1997; Jafari, et al., 1998). In small axons, there was an increase in neurofilament number and density without detectable changes in microtubules, whereas larger axons experienced microtubule loss with either no change or a loss of neurofilament (Jafari, et al., 1997). Differential cytoskeletal alterations in different size axons were seen up to 7 days (final time point) after guinea pig optic nerve stretch (Maxwell, et al., 2003). From our data, optic nerve stretch in the rat resulted in loss of axons regardless of size. Despite an overall treatment effect in the optic nerve core with hypothermia, there was no statistical difference in the density of axons of different sizes between normothermic and hypothermic injured nerves. This may again be due to limited statistical power. Our cross-sectional axonal area measurements may have been overestimates as not all axons were cut perfectly transversely. In spite of this, the data was robust and appeared similar across all four quartiles (Figure 9).

The mechanism of axonal protection with short-duration immediate hypothermia remains to be established. It has been previously demonstrated in animal models of TAI that short-duration hypothermia reduced microtubule loss, prevented alteration in neurofilament structure, and blunted early calpain activity (Büki, et al., 1999; Maxwell, et al., 1999; Sun, et al., 2002). The mechanism is likely multifactorial, and may also include reduction in brain metabolic rate, blockade of excitotoxicity, calcium antagonism, and modulation of the inflammatory response (Sahuquillo and Vilalta, 2007).

Several studies have demonstrated benefit of mild hypothermia after severe TBI in humans (Jiang, et al., 2006; Jiang and Yang, 2007). However, a prospective, multicenter, randomized trial did not show improved outcomes in severe TBI patients treated with mild hypothermia (Clifton, et al., 2001). In that study, the mean time to target temperature was over 8 hours and patient inclusion was based on Glasgow Coma Scale score so brain pathology was likely diverse. In animal models, axonal pathology was seen within minutes of injury and hypothermia was usually instituted immediately (Koizumi and Povlishock, 1998; Büki, et al., 1999; Maxwell, et al., 1999; Sun, et al., 2002). Severe TBI in humans often include axonal injury, as well as focal or more diffuse hemorrhage, with ischemia and ICP elevations as secondary complications. Hypothermia potentially can be modified to target specific pathology. For example, hypothermia targeting refractory ICP elevation can be started hours after injury but must be prolonged for optimal benefit (Jiang, et al., 2006). In our model, we demonstrated that immediate, short-duration hypothermia provided long-term axonal protection.

## Summary

In summary, optic nerve stretch in rats appears to model important phenomena that occur after human TBI. Injury and degeneration of the rat optic nerve mimic the histopathologic changes seen in CNS white matter tracts after human TBI. We were able to demonstrate long-term axonal protection with immediate short-duration hypothermia after TAI using this model.

## Acknowledgements

Research supported by National Institutes of Health grant NS055880 (MM) and the Society of Academic Emergency Medicine Institutional Research Grant (RWN).

## References

Bain AC, Meaney DF. Tissue-level thresholds for axonal damage in an experimental model of central nervous system white matter injury. *J Biomech Eng* 2000;122:615–622. [PubMed: 11192383]

- Bain AC, Shreiber DI, Meaney DF. Modeling of microstructural kinematics during simple elongation of central nervous system tissue. *J Biomech Eng* 2003;125:798–804. [PubMed: 14986404]
- Blumbergs PC, Scott G, Manavis J, Wainwright H, Simpson DA, McLean AJ. Staining of amyloid precursor protein to study axonal damage in mild head injury. *Lancet* 1994;344:1055–1056. [PubMed: 7523810]
- Brodhun M, Fritz H, Walter B, Antonow-Schlorke I, Reinhart K, Zweiner U, Bauer R, Patt S. Immunomorphological sequelae of severe brain injury induced by fluid-percussion in juvenile pigs - effects of mild hypothermia. *Acta Neuropathol* 2001;101:424–434. [PubMed: 11484813]
- Büki A, Farkas O, Doczi T, Povlishock JT. Preinjury administration of the calpain inhibitor MDL-28170 attenuates traumatically induced axonal injury. *J Neurotrauma* 2003;20:261–268. [PubMed: 12820680]
- Büki A, Koizumi H, Povlishock JT. Moderate posttraumatic hypothermia decreases early calpain-mediated proteolysis and concomitant cytoskeletal compromise in traumatic axonal injury. *Exp Neurol* 1999;159:319–328. [PubMed: 10486200]
- Büki A, Okonkwo DO, Wang KK, Povlishock JT. Cytochrome c release and caspase activation in traumatic axonal injury. *J Neurosci* 2000;20:2825–2834. [PubMed: 10751434]
- Chen XH, Meaney DF, Xu BN, Nonaka M, McIntosh TK, Wolf JA, Saatman KE, Smith DH. Evolution of neurofilament subtype accumulation in axons following diffuse brain injury in the pig. *J Neuropathol Exp Neurol* 1999;58:588–596. [PubMed: 10374749]
- Cho KS, Yang L, Lu B, Ma HF, Huang X, Pekny M, Chen DF. Reestablishing the regenerative potential of central nervous system axons in postnatal mice. *J Cell Sci* 2005;118:863–872. [PubMed: 15731004]
- Clifton GL, Miller ER, Choi SC, Levin HS, McCauley S, Smith KR Jr, Muizelaar JP, Wagner FC Jr, Marion DW, Luerssen TG, Chesnut RM, Schwartz M. Lack of effect of induction of hypothermia after acute brain injury. *N Engl J Med* 2001;344:556–563. [PubMed: 11207351]
- Gale SD, Burr RB, Bigler ED, Blatter D. Fornix degeneration and memory in traumatic brain injury. *Brain Res Bull* 1993;32:345–349. [PubMed: 8221124]
- Gennarelli TA, Thibault LE, Adams JH, Graham DI, Thompson CJ, Marcincin RP. Diffuse axonal injury and traumatic coma in the primate. *Ann Neurol* 1982;12:564–574. [PubMed: 7159060]
- Gennarelli TA, Thibault LE, Tipperman R, Tomei G, Sergot R, Brown M, Maxwell WL, Graham DI, Adams JH, Irvine A, Gennarelli LM, Duhaime AC, Boock R, Greenberg J. Axonal injury in the optic nerve: a model simulating diffuse axonal injury in the brain. *J Neurosurg* 1989;71:244–253. [PubMed: 2746348]
- Grady MS, McLaughlin MR, Christman CW, Valadka AB, Fligner CL, Povlishock JT. The use of antibodies targeted against the neurofilament subunits for the detection of diffuse axonal injury in humans. *J Neuropathol Exp Neurol* 1993;52:143–152. [PubMed: 8440996]
- Hirano, A.; Llena, JF. Morphology of central nervous system axons. In: Waxman, SG.; Kocsis, JD.; Stys, PK., editors. *The Axon: Structure, Function, and Pathophysiology*. Oxford University Press; New York: 1995. p. 49-67.
- Jafari SS, Maxwell WL, Neilson M, Graham DI. Axonal cytoskeletal changes after non-disruptive axonal injury. *J Neurocytol* 1997;26:207–221. [PubMed: 9192287]
- Jafari SS, Nielson M, Graham DI, Maxwell WL. Axonal cytoskeletal changes after nondisruptive axonal injury. II. Intermediate sized axons. *J Neurotrauma* 1998;15:955–966. [PubMed: 9840768]
- Jiang JY, Xu W, Li WP, Gao GY, Bao YH, Liang YM, Luo QZ. Effect of long-term mild hypothermia or short-term mild hypothermia on outcome of patients with severe traumatic brain injury. *J Cereb Blood Flow Metab* 2006;26:771–776. [PubMed: 16306933]
- Jiang JY, Yang XF. Current status of cerebral protection with mild-to-moderate hypothermia after traumatic brain injury. *Curr Opin Crit Care* 2007;13:153–155. [PubMed: 17327735]
- Koizumi H, Povlishock JT. Posttraumatic hypothermia in the treatment of axonal damage in an animal model of traumatic axonal injury. *J Neurosurg* 1998;89:303–309. [PubMed: 9688127]
- Levin HS, Williams DH, Valastro M, Eisenberg HM, Crofford MJ, Handel SF. Corpus callosal atrophy following closed head injury: detection with magnetic resonance imaging. *J Neurosurg* 1990;73:77–81. [PubMed: 2352026]
- Maxwell WL, Domleo A, McColl G, Jafari SS, Graham DI. Post-acute alterations in the axonal cytoskeleton after traumatic axonal injury. *J Neurotrauma* 2003;20:151–168. [PubMed: 12675969]

- Maxwell WL, Donnelly S, Sun X, Fenton T, Puri N, Graham DI. Axonal cytoskeletal responses to nondisruptive axonal injury and the short-term effects of posttraumatic hypothermia. *J Neurotrauma* 1999;16:1225–1234. [PubMed: 10619200]
- Maxwell WL, Graham DI. Loss of axonal microtubules and neurofilaments after stretch-injury to guinea pig optic nerve fibers. *J Neurotrauma* 1997;14:603–614. [PubMed: 9337123]
- Maxwell WL, Watson A, Queen R, Conway B, Russell D, Neilson M, Graham DI. Slow, medium, or fast re-warming following post-traumatic hypothermia therapy? An ultrastructural perspective. *J Neurotrauma* 2005;22:873–884. [PubMed: 16083354]
- McCracken E, Hunter AJ, Patel S, Graham DI, Dewar D. Calpain activation and cytoskeletal protein breakdown in the corpus callosum of head-injured patients. *J Neurotrauma* 1999;16:749–761. [PubMed: 10521135]
- Meaney DF. Relationship between structural modeling and hyperelastic material behavior: application to CNS white matter. *Biomech Model Mechanobiol* 2003;1:279–293. [PubMed: 14586696]
- Meaney DF, Smith DH, Shreiber DI, Bain AC, Miller RT, Ross DT, Gennarelli TA. Biomechanical analysis of experimental diffuse axonal injury. *J Neurotrauma* 1995;12:689–694. [PubMed: 8683620]
- Murray CJL, Lopez AD. Alternative projections of mortality and disability by cause 1990–2020: Global Burden of Disease Study. *Lancet* 1997;349:1498–1504. [PubMed: 9167458]
- NIH Consensus Development Panel on Rehabilitation of Persons With Traumatic Brain Injury. Rehabilitation of persons with traumatic brain injury. *JAMA* 1999;282:974–983. [PubMed: 10485684]
- Povlishock JT. Traumatically induced axonal injury: pathogenesis and pathobiological implications. *Brain Pathol* 1992;2:1–12. [PubMed: 1341941]
- Povlishock JT, Katz DI. Update of neuropathology and neurological recovery after traumatic brain injury. *J Head Trauma Rehabil* 2005;20:76–94. [PubMed: 15668572]
- Povlishock JT, Marmarou A, McIntosh T, Trojanowski JQ, Moroi J. Impact acceleration injury in the rat: evidence for focal axolemmal change and related neurofilament sidearm alteration. *J Neuropathol Exp Neurol* 1997;56:347–359. [PubMed: 9100665]
- Saatman KE, Abai B, Grosvenor A, Vorwerk CK, Smith DH, Meaney DF. Traumatic axonal injury results in biphasic calpain activation and retrograde transport impairment in mice. *J Cereb Blood Flow Metab* 2003;23:34–42. [PubMed: 12500089]
- Sahuquillo J, Vilalta A. Cooling the injured brain: how does moderate hypothermia influence the pathophysiology of traumatic brain injury. *Curr Pharm Des* 2007;13:2310–2322. [PubMed: 17692002]
- Sugimoto T, Fukuda Y, Wakakuwa K. Quantitative analysis of a cross-sectional area of the optic nerve: a comparison between albino and pigmented rats. *Exp Brain Res* 1984;54:266–274. [PubMed: 6723847]
- Sun X, Tang W, Zheng L. Ultrastructural observation of effect of moderate hypothermia on axonal damage in an animal model of diffuse axonal injury. *Chin J Traumatol* 2002;5:355–360. [PubMed: 12443577]

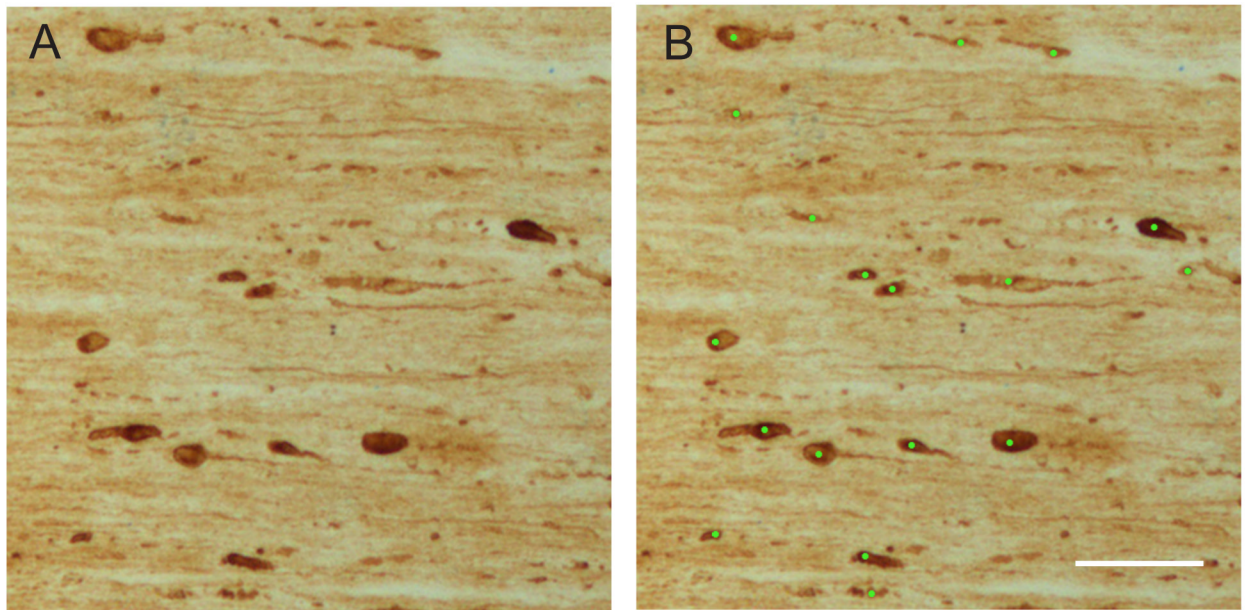


**Figure 1.** Scoring of SMI-32 labeled swellings and bulbs. (A) Ten  $\mu\text{m}$  thick section of an optic nerve from an animal sacrificed 4 days after 8 mm optic nerve stretch. (B) Discrete swellings and bulbs were counted if a circle with a diameter of 2.5  $\mu\text{m}$  were completely contained within their border. Lime green circles have a diameter of 2.5  $\mu\text{m}$ . Scale bar = 50  $\mu\text{m}$ .

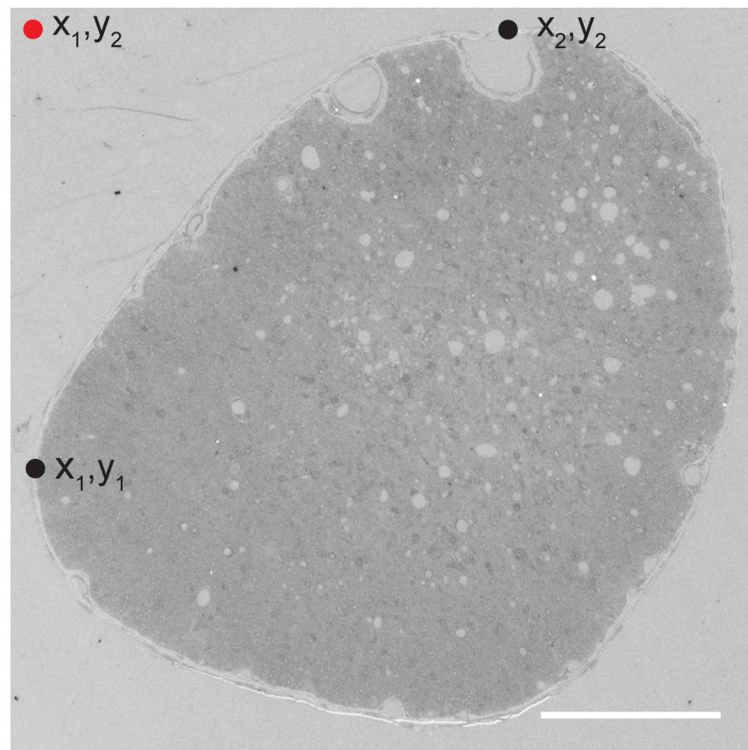


**Figure 2.** Systematic sampling of optic nerve cross-sections using an electron microscope. Coordinates for the most superior ( $x_2, y_2$ ) and leftward ( $x_1, y_1$ ) points of the nerve were established (black dots). The starting point for image capture (red dot) was determined using the  $x_1$  from the most leftward point and  $y_2$  from the most superior coordinate. Images were captured every  $70\ \mu\text{m}$  across and down from the starting point. Disruption of normal architecture is apparent even in this low power image of an optic nerve taken from an animal sacrificed 2 weeks after normothermic 8 mm optic nerve stretch. Scale bar =  $100\ \mu\text{m}$ .

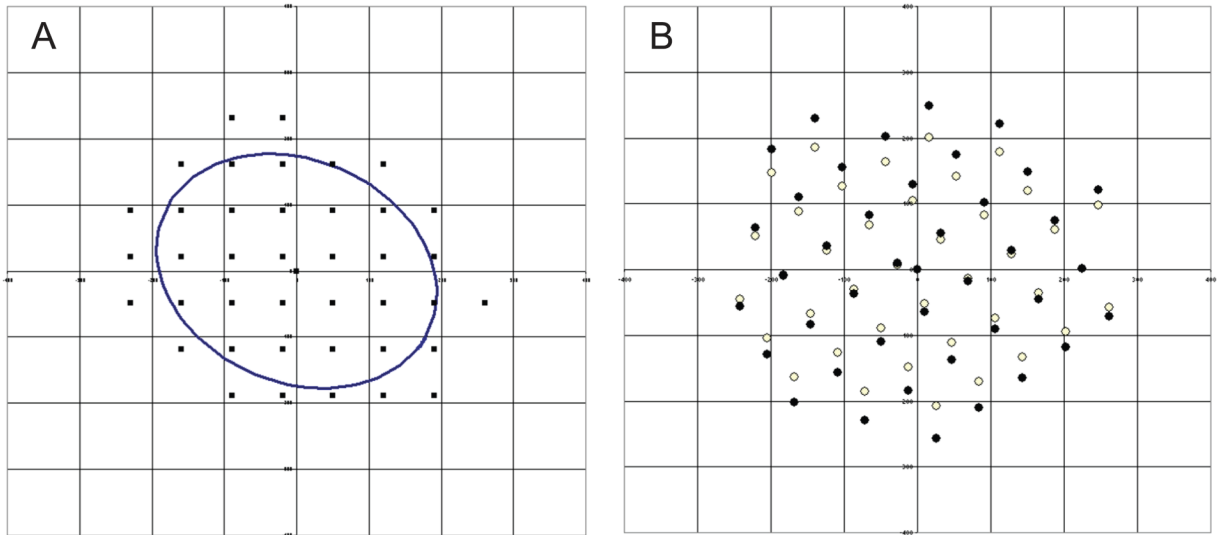


**Figure 3.** Affin transformation of coordinates of electron microscopy images taken from an optic nerve. (A) Idealized ellipse overlay on spatial plot of coordinates. (B) Affine transformation of original coordinates (open circles). Filled circles represent the scaled coordinates.

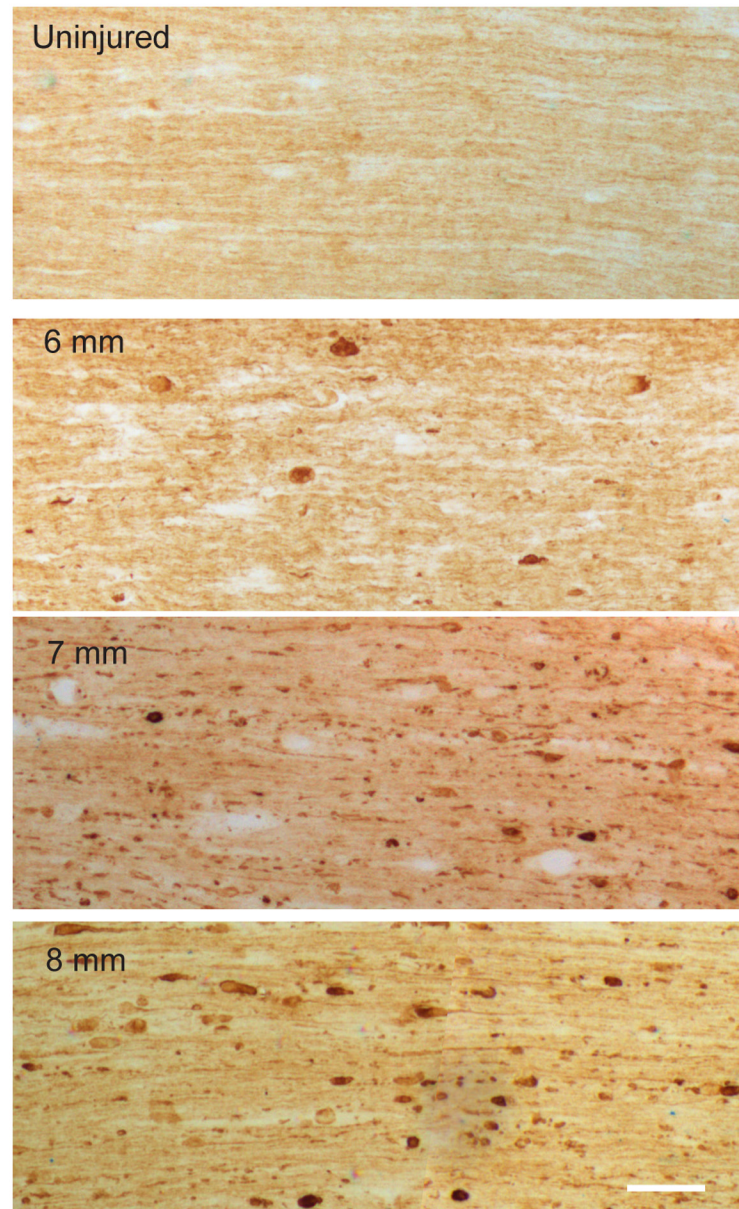


**Figure 4.** Traumatic axonal injury 4 days after optic nerve stretch. SMI-32 immunolabeling of non-phosphorylated neurofilament in 10 μm thick longitudinal sections after 6, 7, and 8 mm optic nerve stretch compared to uninjured (control) optic nerve. Images captured at 100× magnification. Scale bar = 50 μm.

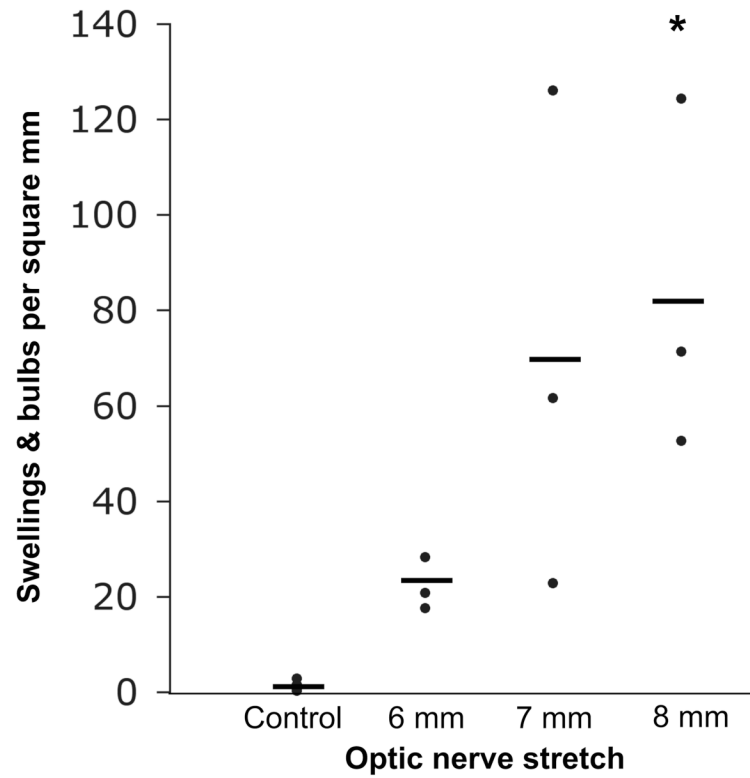


**Figure 5.** Number of swellings and bulbs per square mm in control and injured nerves. Every 8<sup>th</sup> longitudinal section of the optic nerve (10  $\mu$ m thick) was scored. Three nerves in each injury group and the 9 contralateral nerves served as controls. Horizontal bars represent means. \* $p=0.009$  relative to their respective contralateral control optic nerves.

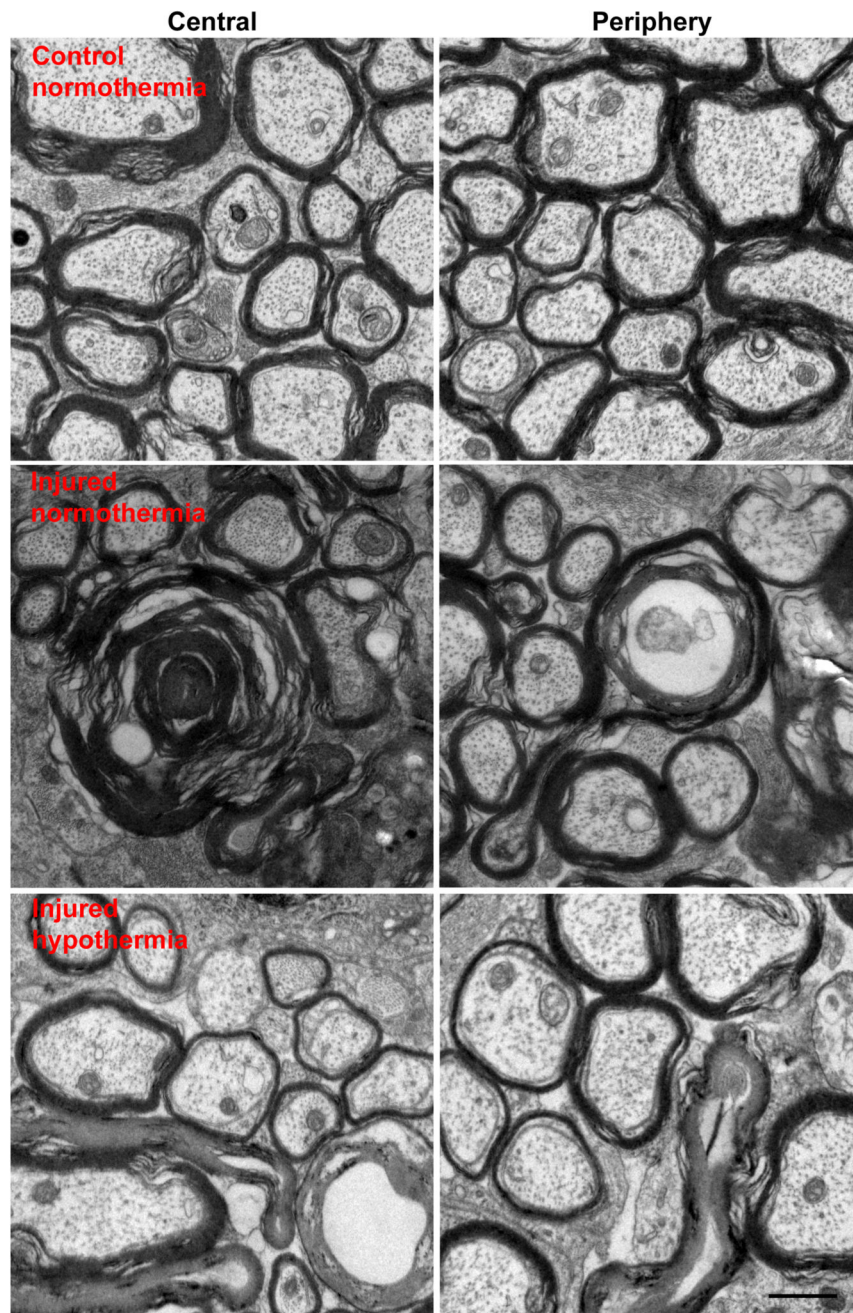


**Figure 6.** Axonal degeneration 2 weeks after 8 mm optic nerve stretch. Representative electron microscopy images taken from the central and peripheral regions of uninjured and injured optic nerves. Images captured at 13,900 $\times$  magnification. Scale bar = 1  $\mu$ m.

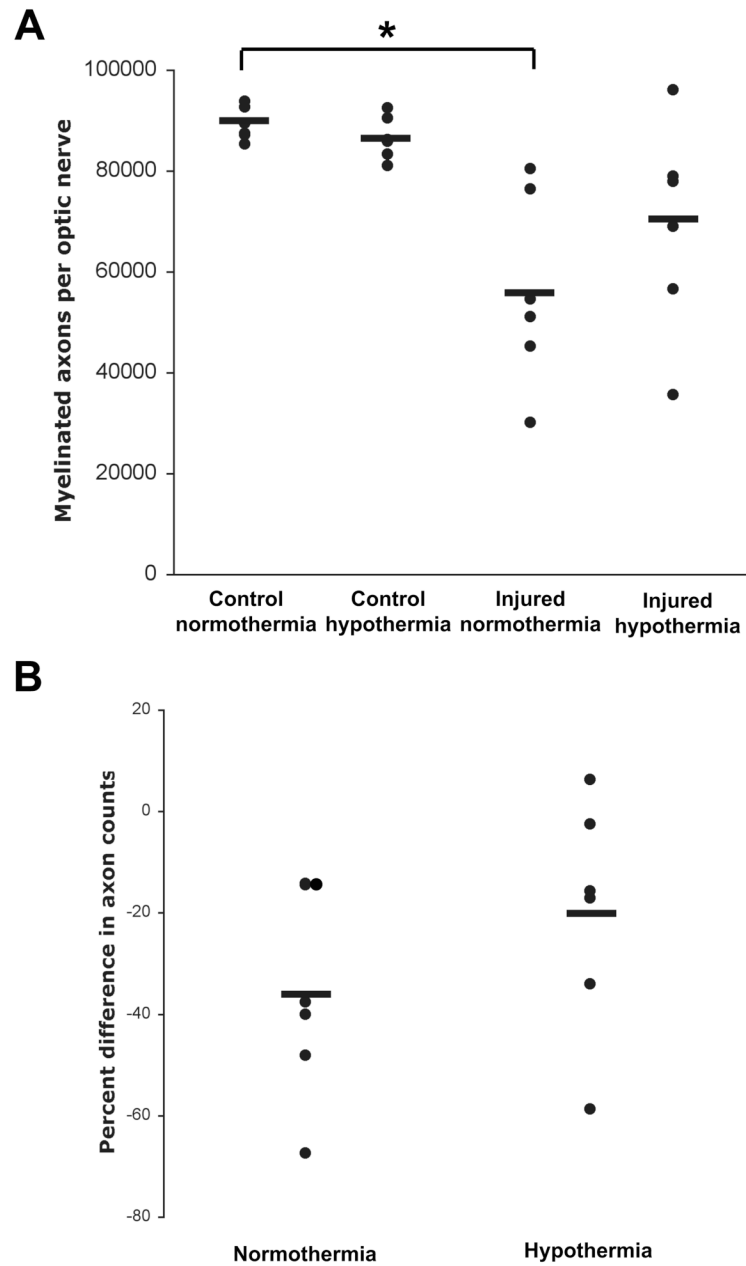


**Figure 7.**

Overall effect of post-injury hypothermia on axonal degeneration. (A) Total axonal counts from control and injured optic nerves from 6 normothermic and 6 hypothermic animals. \* $p=0.002$  when comparing control and injured normothermic groups. (B) Percent difference in total axonal counts between the injured optic nerve and contralateral control nerve. Horizontal bars represent means.

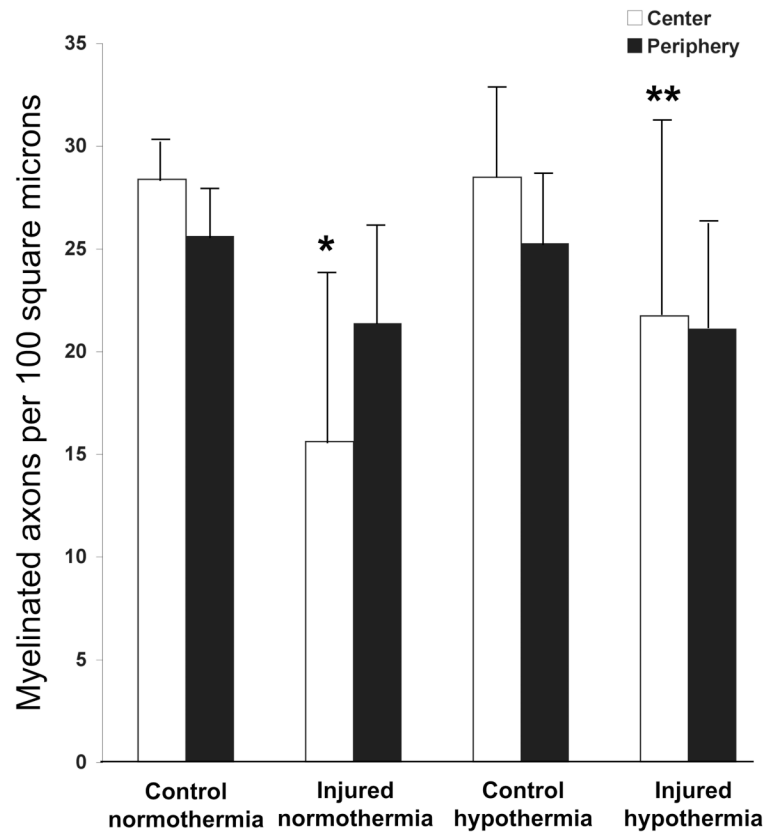


**Figure 8.** Regional effect of post-injury hypothermia on axonal degeneration. Axon densities from control and injured optic nerves from 6 normothermic and 6 hypothermic animals. Error bars represent standard deviation. \* $p < 0.0001$  relative to control normothermia core. \*\* $p = 0.027$  relative to injured normothermia core.

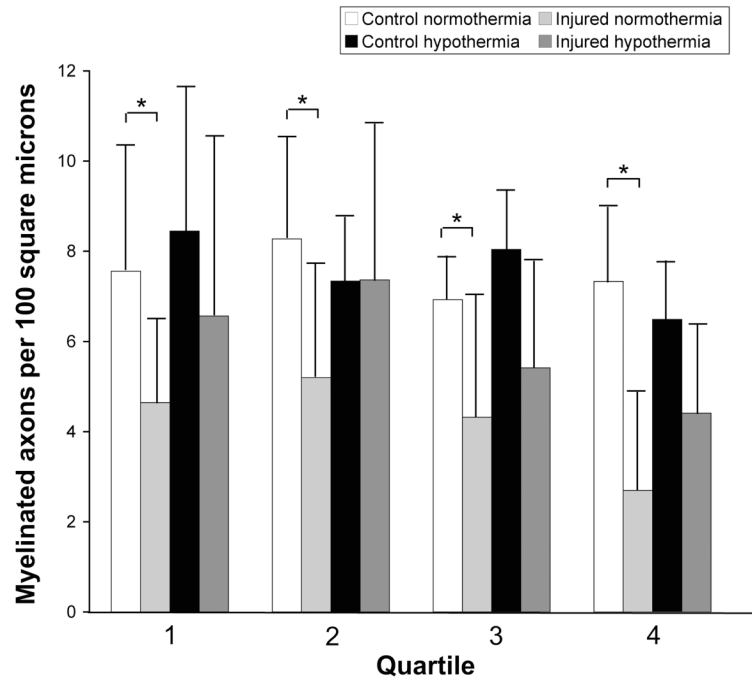


**Figure 9.**

Injury and hypothermic protection based on axon size. Axons with cross-sectional areas less than  $0.56$ , between  $0.56$  and  $0.92$ , between  $0.92$  and  $1.59$ , and greater than  $1.59 \mu\text{m}^2$  are grouped into the first, second, third and fourth quartiles, respectively. Quartiles were based on the size distribution of axons in control normothermic optic nerves. Error bars represent standard deviation. \* $p \leq 0.01$  when comparing control and injured normothermic animals.